

## Effect of Adhesion and Corrosion Performance of Geomet Basecoat (321)- Topcoat (ML Black) Applications on Cathophoretic Coating

İbrahim Usta<sup>1,2\*</sup> , Oğuz Yılmaz<sup>1,3</sup> , Minel Gül<sup>1,4</sup> , Ahmet Can<sup>1</sup> , Harun Gül<sup>2</sup> 

<sup>1</sup>Uzman Kataforez Yüzey Kaplama San. ve Tic. A.Ş., Bursa, Türkiye, b16.ibrahim@gmail.com, oguzyilmaz@uzmankataforez.com, minelgul@uzmankataforez.com, ahmetcan@uzmankataforez.com

<sup>2</sup> Sakarya University of Applied Sciences, Metallurgy and Materials Engineering, Sakarya, Türkiye, b16.ibrahim@gmail.com, harungul@subu.edu.tr

<sup>3</sup> Bilecik Şeyh Edebali University, Chemical Engineering, Bilecik, Türkiye, oguzyilmaz@uzmankataforez.com

<sup>4</sup> Bursa Technical University, Department of Chemical, Bursa, Türkiye, minelgul@uzmankataforez.com

\*Corresponding author

### ARTICLE INFO

### ABSTRACT

#### Keywords:

Cataphoresis  
Geomet  
Zinc Lamellar  
Coating  
Corrosion

#### Article History:

Received: 21.08.2023

Accepted: 05.12.2023

Online Available: 25.02.2024

This study aimed to improve corrosion resistance and adhesion of metallic materials typically used in automotive application. A combination of cathophoretic and Geomet coatings has been used to improve corrosion resistance. Firstly, cathophoretic coating was applied and then the coating process was completed with Geomet 321 and ML Black respectively. The results of the corrosion tests were classified into different categories such as adhesion, water resistance, moisture resistance, salt resistance and cyclic tests. The corrosion properties of the two- and three-layer coatings were found to improve as a function of both the sandblast pre-treatment and the post-cathophoresis curing temperature. The findings show that the adhesion strength and corrosion properties of Geomet 321 increases with curing temperature and sandblasting. This study will be a contribution to the future of protective coatings in the automotive industry by describing the process steps necessary to achieve optimum results.

## 1. Introduction

Metallic materials are widely used in automotive, aerospace, and chemical applications because of their strength, melting point, and hardness. However, corrosion resistance is poor in some metallic materials. Corrosion occurs when metal loses electrons or interacts with air, water, and chemicals. It may also affect the appearance and structural integrity of the metal [1]. Globally, the annual cost of corrosion is estimated to be approximately US \$2.5 trillion [2]. Therefore, improving corrosion properties are an important issue, especially for materials used in corrosive environments [3, 4].

Electrochemical, electrophoretic, galvanic, zinc, chromium, phosphate coatings have been proposed as the best, cheapest and most effective industrial methods of improving metallic corrosion properties [5–11]. Coatings provide a

physical barrier to metal surfaces, extending substrate life [12]. Electroplating and electroless coatings are generally used in the spacecraft and aerospace industry due to their high wear and corrosion properties and high cost [13,14]. Cathophoresis and Geomet coatings offer a more economical option than other coatings, as well as high corrosive resistance. That's why, these coating methods have become increasingly popular in the automotive industry. Cathophoresis coatings are widely used for corrosion protection of metal surfaces. In this method, the metal substrate is immersed in an electrolyte coating bath and an electric current form a thin film [15]. A cathophoretic coating offers an aesthetic appearance, a long service life and resistance to corrosion. Cathophoresis can also be used as a primer before many applications, and superior properties can be achieved with different coating techniques.

**Cite as:** I. Usta, O. Yılmaz, M. Gül, A. Can, H. Gül (2024). Effect of Adhesion and Corrosion Performance of Geomet Basecoat (321)- Topcoat (ML Black) Applications on Cathophoretic Coating, *Sakarya University Journal of Science*, 28(1), 220-236. <https://doi.org/10.16984/saufenbilder.1345904>

Zinc is the most used metal for corrosion protection. It exhibits a lower electrochemical potential than other metals [16–18]. Zinc does not corrode as toxic as cadmium and is suitable for anti-corrosive coatings [19]. The organic zinc lamellar coating (Geomet) is ideal for use in automotive materials. It provides impact, friction, chemical and corrosion resistance for bolts, nuts, hinges, and discs. Therefore, the second and third layers were Geomet 321 and Geomet ML Black after cataphoresis coating. These coatings contain metal oxide, zinc, and lamellar aluminium in their structure [20].

Philip et al. used accelerated corrosion tests (ACT) to investigate the differences between Zn-Fe and Geomet coatings. They observed that Zn-Fe coated screws developed white rust within one week, and after four weeks, significant red rust [21]. However, Geomet-coated screws showed much better corrosion resistance. No rust residues were observed after even eight weeks of exposure to ACT.

Another study compared the corrosion resistance of mechanical, hot-dip and Geomet coatings on a bolt using salt spray. The hot dip and mechanical zinc coatings corroded in a 750-hour corrosion environment while Geomet coatings showed no red-white rusting even after 1000 hours of corrosion [22]. It is also ideal for use on bolted joints, particularly where the bolt is subject to constant friction. It also eliminates the risk of hydrogen absorption associated with many electroplated zinc and zinc alloy coatings. Another advantage over electroplating is that the process is low cost and has significantly less environmental impact [23].

Geomet coatings are completely resistant to inorganic and organic solvents. They provide long term corrosion resistance due to their ability to withstand thermal shock [24]. Geomet coatings have been reported to not only improve the corrosion properties of the bolt coating, but also to provide lubricity, reduce bolt friction and extend service life [22, 25]. In combination with cataphoresis coatings, certain coating types can reduce high wear rates and maximise corrosion

resistance [26]. Non-hydrogen embrittlement lamellar coatings consist of a combination of zinc and aluminium flakes with a water-based inorganic coating. During application, the liquid is applied to the substrate and excess liquid is removed by centrifugal action. A final passivation process enhances the corrosion protection properties of the coating [27].

In this study two different pre-treatment methods, with and without sandblasting, were applied to the surface of the low carbon steel to develop a three-layer corrosion resistant coating process. The first layer was cataphoresis (I), the second layer was base coat (Geomet 321) (II) and the last layer was top coat (Geomet ML Black) (III). To optimise the corrosion resistance, different curing temperatures were used in the cataphoresis process. Adhesion and corrosion resistance of Basecoat 321 and Topcoat ML Black were investigated using water, humidity, salt and cycling tests to assess post-paint corrosion. The combined use of [C+B] and [C+B+T] coatings, the applicability of sandblasting pre-treatment and the effect of different curing temperatures (150, 175, 200, 210, 220, 230 °C) on the coatings were investigated, unlike other studies in the literature. Corrosion resistance was 50% better than other literature studies. The results showed that the best corrosion resistance was achieved with a three-layer coating (C+B+T) in combination with sandblasting pre-treatment and curing at 210°C.

## 2. Experimental Process

### 2.1. Materials

Low carbon steel (AISI 1040) substrates (75x50x5 mm) were used for the experimental coating. All Geomet and Cataphoresis coating chemicals were purchased from PPG and NOF Metal Coating. The coding system shown in Table 1 was used to product 2-layer and 3-layer coatings in the publication. After the necessary pre-treatments, the coatings were applied in two layers [C+B] and three layers [C+B+T].

**Table 1.** Coding of two- and three-layer coatings

COATING TYPE	CODE	LAYER
Cataphoresis+ Basecoat Geomet 321	[C+B]	Two Layer
Cataphoresis+ Basecoat Geomet 321+ Topcoat ML Black	[C+B+T]	Three Layer

To better understand the coating methods used in the paper, both coatings are presented in the form of a model in Figure 1. Figure 1(a) shows the two-layer coating, while Figure 1(b) shows the three-layer coating. All coating procedures and tests were carried out at "Uzman Kataforez San. ve Tic. Ltd. Şti".

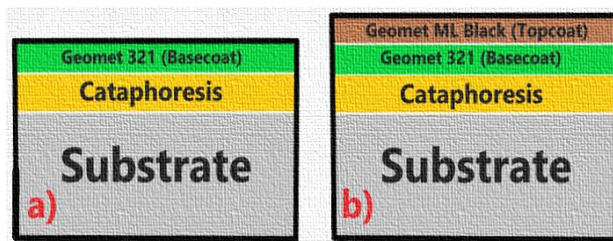


**Figure 1.** Cross-sectional model of the coatings (a: [C+ B] b: [C+ B+ T]).

## 2.2. Method and process

The effect of different curing temperatures applied to the cataphoresis coatings on the adhesion and corrosion properties of Basecoat and Topcoat was investigated. Figure 2 details the surface preparation of the specimens prior to cataphoresis and the application of Geomet Basecoat 321 and Topcoat ML Black. The variable parameters used in the experimental study, sandblasting, and degree of curing, are shown in different colours. Figure 2 shows the coatings applied to the substrate sample from top to bottom. First step two coats [C+B] and then three coats [C+B+T] were applied.

The first step in the pre-treatment process was an acid degreasing process to remove oil and contaminants from the sample surface. This gives the coating a better bond strength and then followed by rinsing and sandblasting.

Two different cataphoresis coatings were produced with the same parameters with and without sandblasting pre-treatment. Sandblasting is a mechanical method of roughening a material surface. Sandblasting can produce nanocrystalline surfaces, just like surface

treatment [28, 29]. Cast steel granular (S-70) powder with a density of 7 g/cm<sup>3</sup> with a hardness of 40-50 HRC was used for the sand blasting process (12A; 10 min. blasting). The cutting action of the abrasive grit completely cleans the surface of the substrate and improves the surface quality. Sandblasting makes the surface rougher and cataphoresis coatings adhere better to the rough surface and provide better adhesion. After sandblasting, rinsing starts again; the necessary pre-treatments are shown in Figure 2.

Activation pre-treatment affects phosphate crystal structure and size [30]. The crystal grains in the coating are thick, especially in zinc phosphate baths. Excessive phosphorus in the coating structure makes the structure porous, greatly reducing corrosion resistance [31]. An activation process is necessary to reduce the size of the phosphate coating crystals. When zinc phosphate crystals are small and thin, a denser and more homogeneous coating forms. Therefore, prior to cataphoresis coating, the activation process plays an essential role in terms of bond strength and corrosion properties.

Phosphating is a process which is widely used for the improvement of corrosion resistance and materials surface structure like steel [31].

The phosphating process creates a thin, rough, and porous layer of phosphate on the surface. This layer ensures that the cataphoresis coating harmonises with the surface. For this reason, phosphating is considered a fundamental step in surface preparation for cataphoresis coating.

The formation of a zirconium passivation layer after phosphating provided greater corrosion resistance by filling the high porosity areas on the sample surface. It also improved the surface properties by increasing the adhesion of the organic coating to be applied (Geomet 321/ML Black). The phosphate film is not uniform on the surface. Passivation homogenises the phosphate and minimises the amount of air that can remain under the cataphoresis. After pre-treatment of the substrate, the first layer of cataphoretic coating was applied. The cataphoresis coating bath was prepared by selecting the concentration and parameters from a previous study [32, 33]. After cataphoresis coating, the paint on the sample surface was filtered twice, and curing processes

were performed at different temperatures (150, 175, 200, 210, 220, 230 °C) for 20 min.

curing window showing various curing times and temperatures at different panel temperatures.

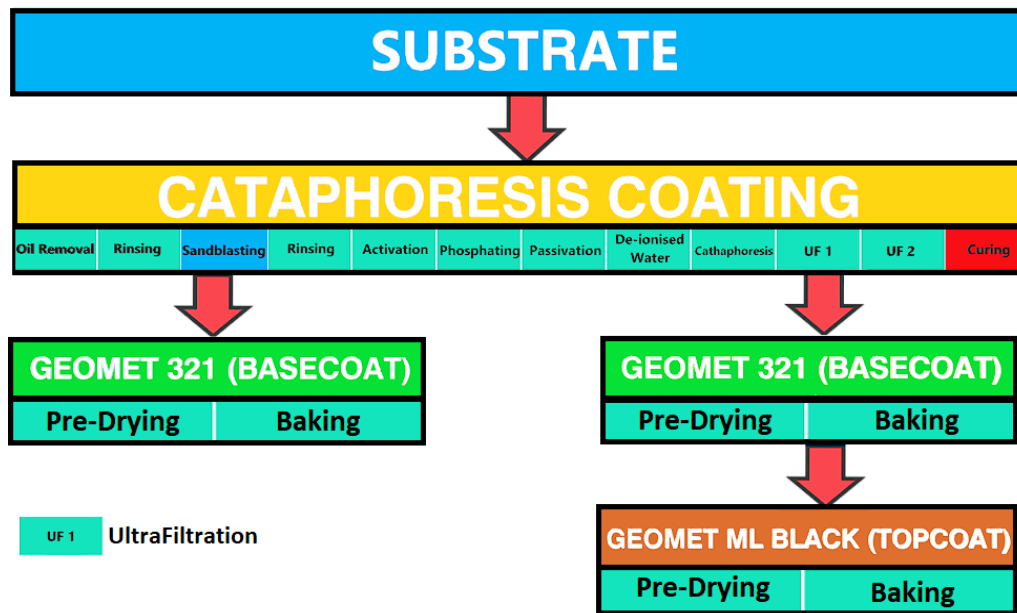


Figure 2. The pre-treatments and coating processes for [C+B] and [C+B+T]

After curing of the cataphoresis coatings, the Geomet coating process was started. Table 2 shows the parameters of the bath for the Basecoat 321 and the Topcoat ML Black coatings.

Table 2. Bath parameters of Geomet 321 and Geomet ML Black coatings

	PARAMETERS	
BASECOAT GEOMET 321	Temperature	20 °C
	Viscosity	90 s (DIN 4 Cup)
	Density	1,32 g/cm <sup>3</sup>
	pH	8
	Solids Amount	%40
PRE-DRYING	Temperature	80-100 °C
	Time	6-10 min.
CURING	Temperature	300-320 °C
	Time	20 min.
	PARAMETERS	
	Temperature	24 °C
	Density	1,10
	Solids Amount	%25
	Coating Time	10 min.
	Temperature	80-100 °C
	Time	6-10 min.
	Temperature	300-320 °C
	Time	20 min.

The NOF chemicals concentration was adjusted using the chemical analyses methods presented by the company to achieve the optimum coating concentration for Geomet coating.

A curing window was used to evaluate the curing quality after cataphoresis. Figure 3 shows a

To produce a quality coating, the values in the curing temperature/time regions containing the inner regions of the red, blue, and black lines should be selected. For example, the curing time at 180 °C should be between 20 and 80 min in Figure 3. The curing window is used to prevent the formation of defects on the surface from being coated.

Increasing the curing temperature after cataphoresis may improve corrosion resistance by providing less permeability on the performance of anti-corrosion primers, or delamination and crack zones may occur due to stress and high hardness [34]. Thus, the degree of curing applied after cataphoresis coating is critical. In addition, a defect on the surface of the cataphoresis coating will adversely affect different types of coating to be applied to it.

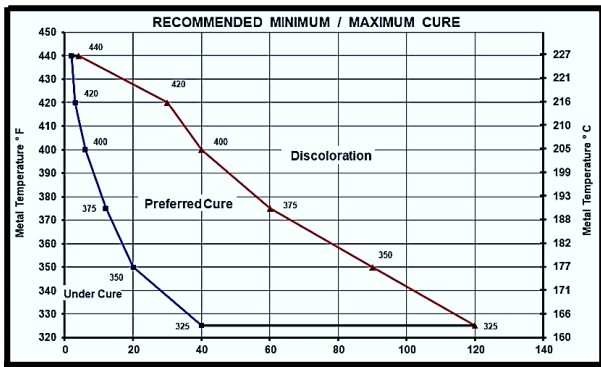


**Figure 3.** Curing window used for determining coating quality after drying [35]

Curing below 155 °C will cause the primer/metallic substrate interphase to become more active, increasing the coating's tendency to delamination. Too low a curing temperature reduces the bond strength of the coating to the substrate. The low binding density increased the delamination areas on the coating surface. The bond density of the coating to the substrate is very fast at very high curing temperatures. The speed of this binding density makes the cathoretic coating more brittle and reduces its corrosion performance [36]. In both cases, the cathoresis coating shows poor performance in corrosive environments. Therefore, the determination of the optimum curing temperature prior to Geomet coating is very important.

After cathoresis coating, Geomet 321 and then Geomet ML Black topcoats were applied on top of each other, using different pre-drying and curing degrees (150, 175, 200, 210, 220, 230) to obtain the optimum corrosion and adhesion result.

### 2.3. Testing process

The thickness of the cathoresis coating was measured using an Elcometer 456 Probe, while the weight of the Geomet coating was measured using a Fischerscope Hybrid System X Ray instrument. Contact angle measurements were performed with Theta Flex Contact Angle Measurement Device. Each sample was photographed with Canon EOS 600D camera for comparison of sample images after the test.

All the post-coating tests are shown in Figure 4. Adhesion testing is generally used to determine the bond strength and the force required to peel the coating from the substrate on surfaces such as painted surfaces. All samples were tested using a Qualtech Cross Cutting Tester (REF DIN ISO 2409) (6-blade system at 1mm pitch). Tests were performed at room temperature,  $50 \pm 5\%$  relative humidity and constant pressure, with a tape width of 25 mm and an adhesive force of 6 - 10 N on glass. In the adhesion test, the coating surface to be tested is first cleaned and degreased, then cut

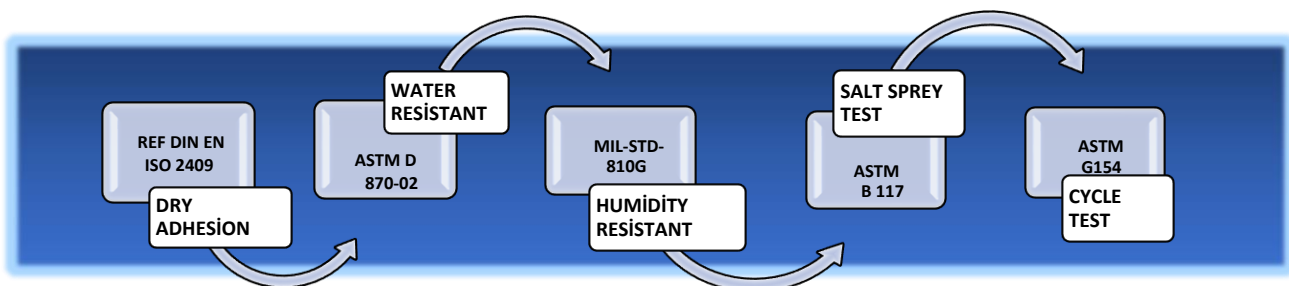


**Figure 4.** Tests applied after coatings are produced

Geomet 321 coatings were applied for 10 minutes at room temperature, pH 8. The speed of the centrifuge was 280 rpm for Geomet coatings. The Geomet 321 coatings were pre-dried at 90 °C and curing at 300 °C for 30 minutes. The application of the coating was carried out for 10 minutes at room temperature. The pre-drying and curing parameters used for the [C+B] coating was applied to the [C+B+T] coating, and the coatings were prepared for testing.

with a sharp tool (knife, razor blade) down to the substrate material (two cuts at 30-45°) to create edges where the coating can be removed.

Adhesive tape is applied over the cut area and pressed to the coating surface diagonally along the pattern. The tape is then pulled back in a parallel direction to the surface. When the coating peels off because of removing the tape; it will be concluded that the coating adhesion strength is insufficient.

The test area is visually inspected, and the adhesion strength is graded based on the amount of peel from the substrate surface [37]. Figure 5 shows a detailed model of the peel test.

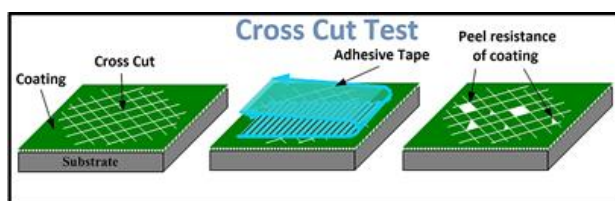


**Figure 5.** Cross-Cut Band Test Model [38]

The degree of peeling of coatings can be determined according to the ISO standard shown in Table 3. ISO 0-5 represents the peel rates of the coatings from the best to the worst.

Dry adhesion tests were first carried out on Geomet 321, and Geomet ML Black coatings pre-treated with and without sandblasting. The samples that passed the dry adhesion test were subjected to water and moisture resistance testing and then adhesion testing. After these tests, the adhesion and corrosion properties of the coatings were investigated by performing salt spray and cycle tests on the coatings that passed the adhesion test. Table 4 shows all tests and parameters. All adhesion tests were scored using the conditions shown in Table 3. "0" and "1" were considered successful and tested further, while "2", "3", "4" and "5" were considered failed and not tested further.

**Table 3.** Conditions for evaluating the amount of peeled coating after the Cross-Cut Tape Test [37]

Peel Type	Definition	Peel Degree
	Perfectly straight cut edges. No abrasions on the coating.	0
	Flaking of coatings in the crosscut mid-section. Less than 5%, no significant peeling visible.	1
	Intermediate areas and edges of the coating have peeling. (5- 15%)	2
	Partial or total breakage along the peel edges, partial or total breakage of individual pieces in wide strips and trims (15-35%).	3
	Partial or total breakage of wide strips or individual squares. (35-65%)	4
	Over 65% peel of coating from surface.	5

The water resistance tests (according to ASTM D 870-02 standard) of the coating samples produced within the scope of the study were

carried out in a BM 402 water bath (Figure 6) [39]. The samples were kept in deionised water at a constant temperature of  $60\pm 2^\circ\text{C}$  in a water bath for 24 hours. After 24 hours, samples were removed from water bath and dried. Samples were kept at room temperature for two hours and adhesion tested. As a result of the peel test, no deformation (peeling) and no change in coating colour is expected.

The moisture resistance of the coating samples was also examined in a hot atmosphere (according to MIL-STD-810G Method 507.5) using a BM 402 water bath (Figure 6) [40]. It is relatively important for applications where the coating material is exposed to changes in different pressure or temperature.

**Table 4.** Test and parameters performed after coating

Test	Device	Temperature	Time (hours)
Water Resistant	BM 402	$60 \pm 2^\circ\text{C}$	24h
Humidity Resistant	BM 402	$40\pm 1^\circ\text{C}$	150h
Salt Spray (%5 NaCl)	ASCOT	$35^\circ\text{C}$	1000h at 24h intervals
Cycle Test	Scania/STD4319	$35^\circ\text{C}$	A single cycle lasts for 24h and there are 63 cycles to be completed (1512h.) (Fig 7).

This is because moisture in the atmosphere can react with the metal components on the coating, which can disrupt the coating integrity structure. To determine the moisture resistance, moisture testing was performed on the produced samples. Moisture can cause oxidation of the coating structure and chemical or electrochemical degradation of organic and inorganic surface coatings. The coating sample was kept at  $40^\circ\text{C}$  for 150 h for the moisture test.



**Figure 6.** Water and moisture resistance test (BM 402)

The resistance of a coating to corrosive environments is evaluated by salt spray testing. This test is performed by spraying salt on the coating surfaces placed in the test chamber and observing the corrosive effect on the material and the corrosion process. To ensure the correct application of this test, the ISO 9227 has been implemented in the ASTM B 117 standard [41]. The study used ASCOT as a corrosion chamber. The salt spray test creates a highly corrosive atmosphere using a standard 5% NaCl solution.

After testing, surface corrosion is evaluated according to standards and acceptance criteria. At the end of the test, the surface is expected to be free from staining, deformation, red rust (a max. of 5% rust [42].) and white rust due to corrosion. Figure 7 shows the cabinet in which the salt spray and corrosion cycle tests are conducted.

A method of evaluating the performance of a coating in a corrosive environment is corrosion cycle testing. It is then subjected to a series of temperature, moisture, and chemical tests. Cycle testing is performed using the Scania/STD4319 device according to ASTM G 154 and lasts 24 hours. A total of 63 cycles are completed by returning to the start after five repetitions. The parameters used in the cycle tests are detailed in Figure 8. These cycles evaluate coating material durability by examining corrosion, rusting and other material effects. After corrosion cycles, specimens are inspected for corrosion severity, coating quality, surface deformation, and other characteristics.



**Figure 7.** Cabinets for salt spray test (a) and cycle tests (b)

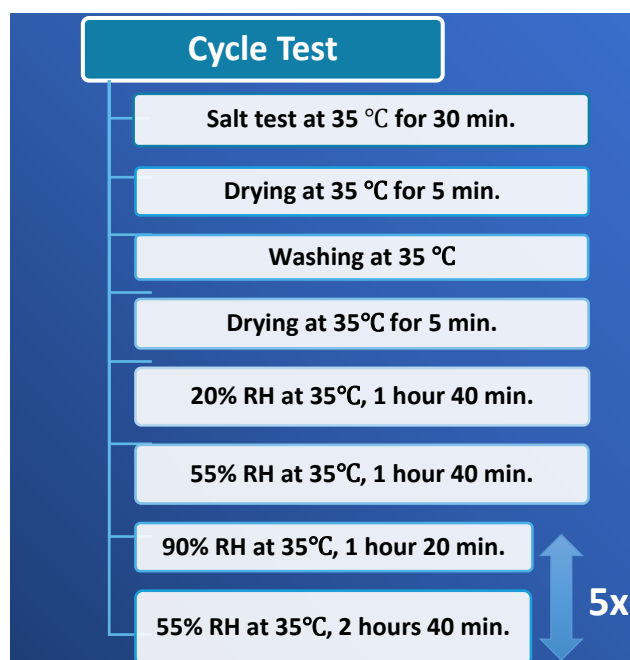


**Figure 8.** Cycle test parameters applied to coatings.

### 3. Conclusions and Discussion

It was observed that the average coating thickness after cataphoresis coating was 20  $\mu\text{m}$ . The amount of coating per  $\text{m}^2$  after Geomet coatings was obtained by dividing the weight difference before and after coating by the surface area. Densities of Geomet Basecoat and ML Black are presented in Table 5 as  $\text{g}/\text{m}^2$ . Because of Geomet coatings are dip-spin processes, a homogeneous coating is not formed on the surface and therefore the coating thickness is given in gram per  $\text{m}^2$ . For visual inspection, images of (a) C+B (white) and (b)C+B+T (black) samples after coating are shown in Figure 9.

**Table 5.** Geomet 321 and ML Black coating density ( $\text{g}/\text{m}^2$ )

Curing Degree ( $^{\circ}\text{C}$ )	Geomet 321 ( $\text{g}/\text{m}^2$ ) (Basecoat)	ML Black ( $\text{g}/\text{m}^2$ ) (Topcoat)
150	15.1	2.64
175	18.8	2.14
200	17.5	1.87
210	26.3	2.14
220	20.4	2.34
230	18.2	1.25

Firstly, surface images of Geomet 321 (Basecoat) were examined in Figure 9. The adhesion strength of Geomet 321 is low due to the low curing temperatures of 150 and 175 $^{\circ}\text{C}$  after cataphoresis. This is because the low curing

temperature creates delamination areas in the coating. As a first observation, curing at higher temperatures gives better adhesion to Geomet 321. Good adhesion was observed at all curing temperatures prior to Geomet ML Black (Topcoat) testing.

problem, and the sample was prepared for the next test.

Figure 10b shows the surface images of Geomet 321 coatings without sandblasting pre-treatment after dry adhesion test. Comparing the Geomet 321 coatings with and without sandblasting pre-

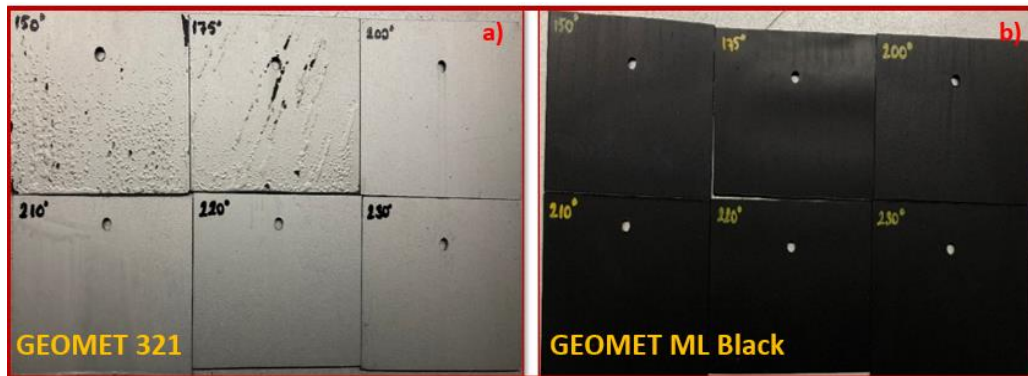


Figure 9. Surface images of after coating. (a: C+B b: C+B+T)

### 3.1.Dry adhesion test

The dry adhesion tests were carried out without any post coating corrosion test. Figure 10a shows the images of sandblasted C+B coatings after dry adhesion test. Table 6 shows the degree of peeling of Geomet 321 (Basecoat) coatings. The amount of peeling decreased with increasing curing temperatures. A high degree of peeling of the coating was clearly visible at a curing temperature of 150°. The coatings curing at 175, 200, 210, 220° were unsuccessful, although the amount of coating passing to the tape decreased with increasing curing temperatures. The coating curing at 230° has not been observed any peeling

treatment, the first impression is that the adhesion of the sandblasted samples is much better. In particular, the coatings at 150, 175 and 200° cured without sandblast pre-treatment were judged unsuccessful in the dry adhesion test due to excessive peeling. No peeling was observed at 210° curing temperature, and the test was therefore successfully passed.

Due to the low peel of the coatings, the samples treated at 220° and 230° were also eliminated. As a result, all second layer samples [C+B] that were not sandblasted except 210° were eliminated in the adhesion test.

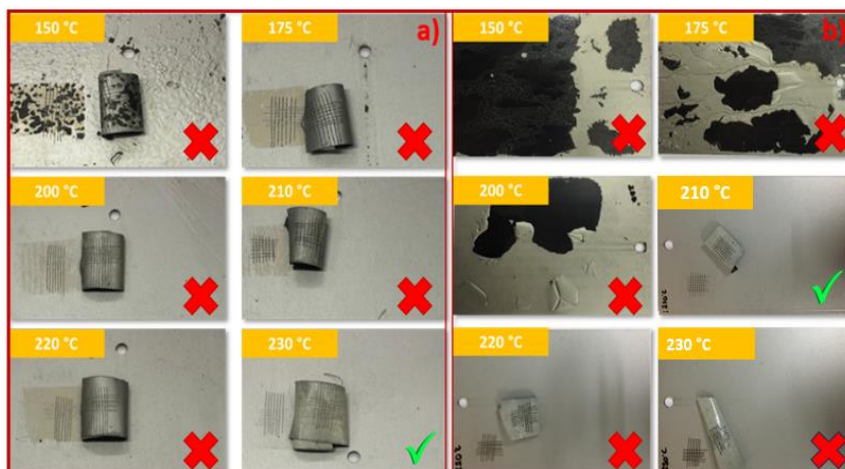


Figure 10. Surface images of Geomet 321 (Basecoat) coatings with different degrees of cure after cathaphoresis coating with (a) and without (b) sandblasting pre-treatment after dry adhesion test

**Table 6.** Dry adhesion test results of Geomet 321 (Basecoat) coatings with different degrees

Coating Type	Sandblasting Pre-treatment	Curing Degree (°C)	Peel Degree	Test Results
CATAPHORESIS + GEOMET 321 (BASECOAT)	APPLIED	150	5	FAIL
		175	4	FAIL
		200	3	FAIL
		210	3	FAIL
		220	3	FAIL
		230	0	PASSED
	NOT APPLIED	150	5	FAIL
		175	5	FAIL
		200	4	FAIL
		210	0	PASSED
		220	2	FAIL
		230	3	FAIL

Due to the low peel of the coatings, the samples treated at 220° and 230° were also eliminated. As a result, all second layer samples [C+B] that were not sandblasted except 210° were eliminated in the adhesion test.

dry adhesion test and were approved for water resistance testing. It can be said that the dry adhesion strength of ML Black topcoats is much higher than C+B coatings at all curing temperatures.

This is due to the silicate material contained in the ML Black coating. Zinc based coatings offer a higher level of adhesion due to their formation with an epoxy resin binder and an inorganic silicate [43]. Silicate material has been reported to be a good binder in previous studies [44]. In addition, reducing the grain size of the coating material can both improve the properties of the coating and provide better adhesion of the coating to the surface as a suitable binder [45]. Determination of solid-liquid interfacial tensions is essential in terms of corrosion properties. For this reason, contact angles of Geomet ML Black

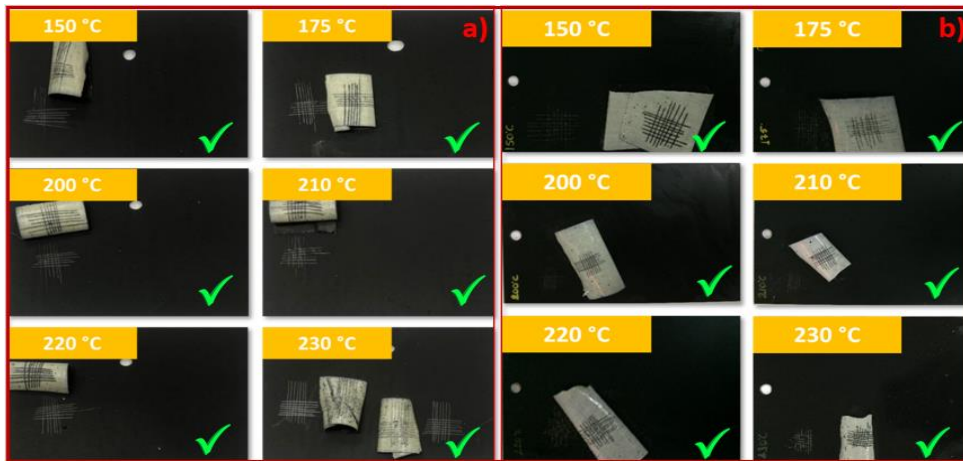


**Figure 11.** Surface images after dry adhesion test of Geomet 321 + ML Black coatings produced at different degrees of cure after cataphoresis coating with (a) and without (b) sandblasting

The images after the dry adhesion tests of C+B+T coatings with sandblasting pre-treatment at different curing degrees are presented in Figure 11a, and the test results are presented in Table 7.

The coatings passed the dry adhesion test at all curing temperatures. ML Black coatings were found not to peel from the surface and to adhere well when all surface images were analysed.

Figure 11b shows the surface images of Geomet ML Black coatings without sandblasting pre-treatment and with different degrees of curing. As with sandblasted coatings, no peeling was observed at all cure levels; all samples passed the

(Topcoat) coatings were measured before water, humidity, salt fog and cycling tests.

**Table 7.** Dry adhesion test results of C+B+T coatings with different degrees of cure after cataphoresis

Coating Type	Sandblasting Pre-treatment	Curing Degree (°C)	Peel Degree	Test Results
CATAPHORESIS + GEOMET 321 (BASECOAT) + GEOMET ML Black (TOPCOAT)	APPLIED	150	1	PASSED
		175	1	PASSED
		200	0	PASSED
		210	0	PASSED
		220	0	PASSED
		230	1	PASSED
	NOT APPLIED	150	1	PASSED
		175	1	PASSED
		200	1	PASSED
		210	0	PASSED
		220	0	PASSED
		230	1	PASSED

Contact angle measurements were performed with Theta Flex Contact Angle Measurement Device. The contact angle is determined according to a certain standard in a material where corrosion resistance is required. Typically, the aim is to create a hydrophobic (water-repellent) effect on the coating surface to improve corrosion resistance. This is the way in which a drop of water spreads or collects on the surface of a material [46]. Increasing the contact angle allows the water droplet to spread and flow more, rather than collecting in a small area on the surface. Therefore, the effect of after coating curing on the contact angle was investigated.

Figure 12 shows a graph of the contact angles on the coating surface. This shows a progression from a spreading (most wettable) to a non-wetting contact angle with increasing contact angle. Increasing the contact angle reduces the liquid penetration on the coating sample surface. It increases the corrosion resistance of coatings by reducing the surface defect/corrosion rate that will occur over time [47].

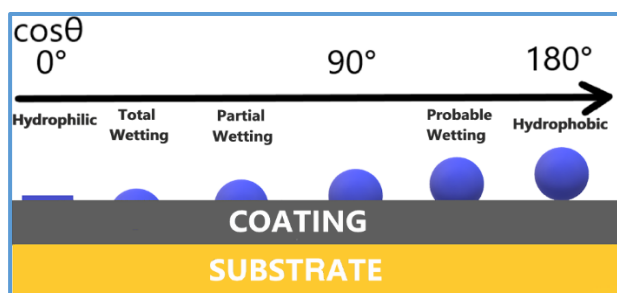


**Figure 12.** Hydrophobicity and hydrophilicity varying with contact angle. (Adapted from Tylkowski B. and Tsibranska I.) [47].

The contact angles of the coatings increased according to the contact angle of the substrate. The contact angle of the low carbon steel substrate was reported to be  $49.5^\circ$  in previous studies [48]. Compared to the contact angles after coating and substrate, the contact angles increased by an average of 42% according to substrate (Figure 13). It can be said that the coatings tend from a hydrophilic to a hydrophobic structure with an increase in the contact angle. This increased contact angle reduced liquid retention on the coating surface and improved corrosion resistance. The coating samples were observed to increase to a contact angle of  $73^\circ$  with an increasing degree of curing.

A whole wetting angle is observed in the substrate, and a partial wetting angle is observed in the coatings when this contact angle is evaluated on the graph. This result proves that the coating with high wetting angle provides the best corrosion properties.

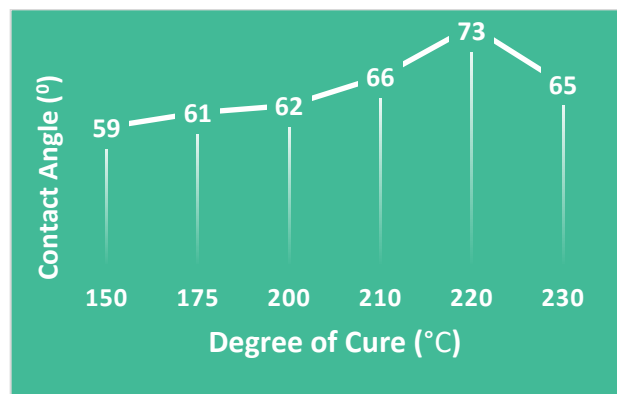


**Figure 13.** Effects of curing degrees after cataphoresis on coating contact angles (C+B+T)

### 3.2. Water resistance test

After the water resistance test, adhesion tests were performed on the with (a) without (b) sandblasted C+B+T and C+B (indicated in yellow) coatings produced at different curing temperatures and their surface images are presented in Figure 14. Table 8 shows the adhesion test results graded according to the standard. After the water resistance test, the samples produced at 150, 175, and 200 curing degrees in sandblasted (a) coatings after the water resistance test have not been pass the test as some of the coating layer passed into the adhesion band after the adhesion test. It was concluded that this situation affected the adhesion resistance due to the low bond density of the coatings on the substrate surface at low curing temperatures.

No peeling was observed at 210 and 220° curing degrees and these samples passed the test. In the case of the non-sandblasted coatings, the samples produced at high cure rates (210° (C+B), 220°(C+B+T) were not stripping from the surface after the water test and prepared for the moisture resistance test. The non-sandblasted coatings at 150, 175 and 200° curing failed the adhesion test after the water test. The coatings peeled off the surface at low curing temperatures with a water resistance effect. According to the

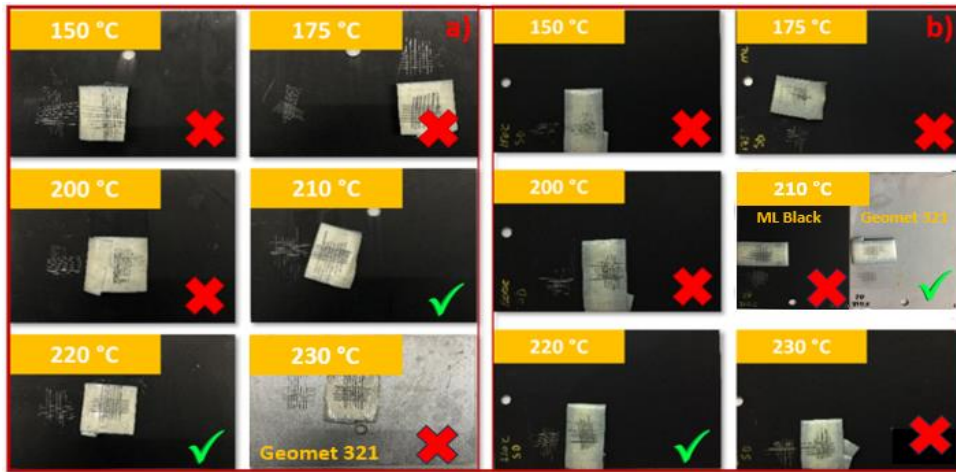


Figure 14. C+B+T (three layer) coatings surface image of after water resistance

test results, curing temperatures above 200°C increased corrosive performance and adhesion resistance. However, there was surface shrinkage due to rapid drying and a reduction in bond strength when cured at 230°C with and without sandblasting.

Table 8. Adhesion test results after water resistance of Geomet ML Black

Coating Type	Sandblasting Pre-Treatment	Curing Time (°C)	Peel Degree	Test Results
CATAPHORESIS + GEOMET 321 (BASECOAT) + GEOMET ML Black (TOPCOAT)	APPLIED	150	3	FAIL
		175	2	FAIL
		200	2	FAIL
		210	1	PASSED
		220	0	PASSED
		230	4	FAIL
		230 (Geomet 321)	4	FAIL
	NOT APPLIED	150	3	FAIL
		175	3	FAIL
		200	2	FAIL
		210	3	FAIL
		210 (Geomet 321)	1	PASSED
		220	0	PASSED
		230	2	FAIL

### 3.3. Moisture resistance test

In order to investigate the reaction of the sandblasted (a) and non-sandblasted (b) coatings in a hot and humid atmosphere, a moisture resistance test was carried out on Geomet 321 and Geomet ML Black coatings. The tape adhesion tests of the coatings with (a) and without (b) sandblasting after moisture resistance test is presented in Figure 15. The adhesion test results determined according to the standard are given in Table 9.

Table 9. Adhesion test results after moisture resistance of Geomet ML Black coatings

Coating Type	Sandblasting Pre-treatment	Curing Degree (°C)	Peel Degree	Test Results
CATAPHORESIS + GEOMET 321 (BASECOAT) + GEOMET ML Black (TOPCOAT)	APPLIED	210	0	PASSED
		220	4	FAIL
	NOT APPLIED	210 (Geomet 321)	0	PASSED
		220	0	PASSED

After the moisture resistance test, the sandblasted C+B+T coating curing at 220° failed the moisture resistance test, while the curing at 210° and passed the test successfully. This is because to the brittle structure of the coatings after cataphoresis with the increase in bond density with high curing temperature. In addition, the surface contact area decreases with the increase in the lamellar structure of Geomet coatings [49]. The 2-layer [C+B] and 3-layer [C+B+T] coatings at 210° without sandblasting pre-treatment passed the test. Curing at 220° without sandblasting [C+B+T], coatings passed the test, and the samples that passed the test were prepared for salt testing.

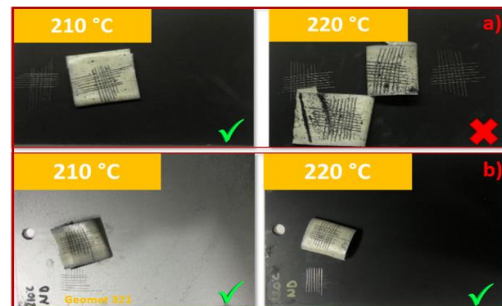
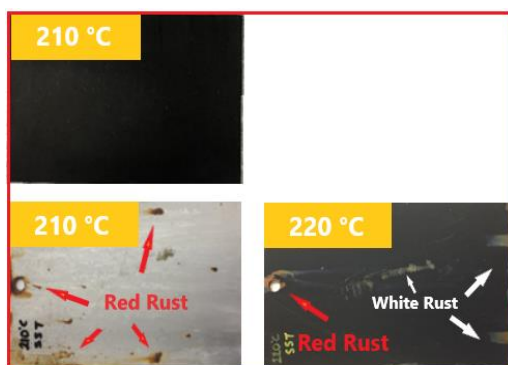


Figure 15. Adhesion test surface images of Geomet ML Black coatings with (a) and without (b) sandblasting after moisture resistance

### 3.4. Salt spray test

Illustrated in Figure 16 are the surface images after the salt test, depicting coatings both with (a) and without (b) prior to sandblasting pre-treatment. Following the conclusion of the test, an absence of corrosion indications was noted on the ML Black topcoat, which had undergone curing at 210° after the cataphoresis process. The cataphoresis + Geomet 321 coating cured at 210°, and the ML Black topcoat cured at 220° failed this test due to corrosion. The non-sandblasted Geomet 321 coating at 210°C has not been pass the salt test due to the formation of too many red rust patches. Due to the formation of red and white rust patches, the non-sandblasted ML Black coating surface (220) also failed the test.



**Figure 16.** Surface images of Geomet ML Black coatings with (a) and without (b) sandblasting after salt test

### 3.5. Cycle test

The surface image of C+B+T coating curing at 220° after sandblasted cataphoresis coating is given in Figure 17a. The surface images of the 321-coating curing at 210° without sandblasting and the C+B+T coating curing at 220° are presented in Figure 17b. Since the cycle test is more aggressive than the salt test, C+B curing at 210° and Topcoat Geomet ML Black coating

curing at 210, and 220° were retaken into the cycle test after the salt test.

The best corrosion performance was obtained by curing at 210 and 220°C. The basecoat Geomet 321 coating without sandblasting passed the cycle test as no red rust formation was observed, although white rust residue was formed at 210°C curing condition. Topcoat ML Black coatings curing at 210°C with sandblasting and 220°C without sandblasting successfully passed the cycle test as no red rust formation was observed. As a result, all the coating samples shown in Figure 17 passed the cyclic corrosion test for 1512 hours.

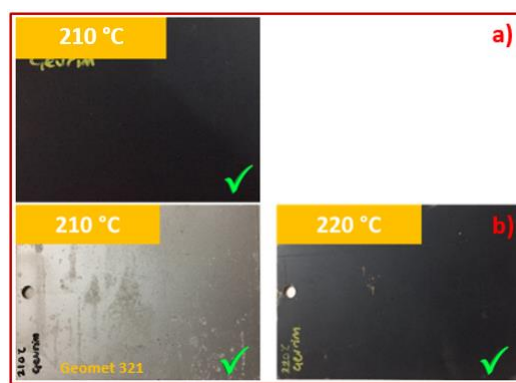


**Figure 17.** Post-cycle surface images of C+B+T coatings

The cycle results of the zinc coatings, Geomet coating, and the results obtained in the study after the salt test are shown in Table 10 for comparison with the study. According to these results in the literature, alkaline Zn, Zn-Fe, and Zn-Ni coatings withstood the cyclic salt test for 300 hours, 360 hours, and 720 hours, respectively [50, 51]. These values were increased to 1008 hours with more innovative Geomet coatings. In this study, Basecoat 321 and Topcoat ML Black coatings applied on cataphoresis have not been observed red and white rust formation even in the 1512 hours (63 cycles) salt test. It was concluded that

**Table 10.** Comparison of corrosion properties of coating after Salt Spray

	Alkaline Zn Coating [50]	Alkaline Zn-Fe Coating [50]	Alkaline Zn-Ni Coating[50]	Cataphoresis Coating [51]	[Basecoat 321] + [Topcoat ML Black] [52]	[Cataphores] + [Basecoat 321] + [Topcoat ML Black] (This paper)
Corrosion Resistance	300 hours	360 hours	720 hours	720 hours	1008 hours	1512 hours
Cyclic Corrosion Resistance	13 cycles	15 cycles	30 cycles	30 cycles	42 cycles	63 cycles

the cathaphoretic intermediate coat applied prior to the Geomet coating increased the corrosion resistance of the Geomet (321 + ML Black) coatings by 50 percent.

As a result, Cataphoresis and Geomet coating, which have superior corrosion resistance, were deposited together on a similar substrate, resulting in much higher corrosion resistance to corrosion environments.

Low curing temperatures which led to delamination and reduced bond strength. The first test applied to the coating samples, water resistance, was successful at 210 and 220 °C. The coating layer shrinkage due to rapid drying and had a brittle structure at the high curing temperature (230°C).

In addition, the rapid drying of the cataphoresis coating resulted in a rough and inhomogeneous

**Table 11.** Comparative test results of [C+B] and [C+B+T]

		✓	Samples passing the test					
		X	Sample that failed the test					
		-	Untested sample (Sample that failed to pass the previous test)					
Coating Type	Sandblasting Pre-treatment	Cure Degree (°C)	Dry Adhesion Test	Water Resistant Test	Moisture Resistance	Salt Test	Cycle Test	RESULT
Cataphoresis + GEOMET 321 (2 Layer)	APPLIED	150	X	-	-	-	-	FAIL
		175	X	-	-	-	-	FAIL
		200	X	-	-	-	-	FAIL
		210	X	-	-	-	-	FAIL
		220	X	-	-	-	-	FAIL
		230	✓	X	-	-	-	FAIL
	NOT APPLIED	150	X	-	-	-	-	FAIL
		175	X	-	-	-	-	FAIL
		200	X	-	-	-	-	FAIL
		210	✓	✓	✓	X	✓	PASSED
		220	X	-	-	-	-	FAIL
		230	X	-	-	-	-	FAIL
Cataphoresis + GEOMET 321 + ML Black (3 Layer)	APPLIED	150	✓	X	-	-	-	FAIL
		175	✓	X	-	-	-	FAIL
		200	✓	X	-	-	-	FAIL
		210	✓	✓	✓	✓	✓	PASSED
		220	✓	✓	X	-	-	FAIL
		230	✓	X	-	-	-	FAIL
	NOT APPLIED	150	✓	X	-	-	-	FAIL
		175	✓	X	-	-	-	FAIL
		200	✓	X	-	-	-	FAIL
		210	✓	X	-	-	-	FAIL
		220	✓	✓	✓	X	✓	PASSED
		230	✓	X	-	-	-	FAIL

Analysing the dry adhesion results in Table 11, Geomet ML Black topcoat shows much better adhesion than Geomet 321 basecoat. This is due to the silicate material in the Geomet ML Black topcoat. The sandblast effect was positive for the topcoats, while it was negative for the 321 coatings. According to corrosive test results, increasing curing temperatures obtained good results for both two- and three-layer coatings.

structure, which adversely affected the corrosion properties due to the uneven deposition of the Geomet coatings on the surface.

#### 4. Conclusion

In summary, the study evaluated the performance of the Geomet coatings, specifically the Geomet 321 basecoat and the Geomet ML Black topcoat, applied by means of a cataphoresis process. The results showed that the adhesion strength of

Geomet 321 is influenced by the curing temperature, with higher temperatures resulting in better adhesion. Dry adhesion tests showed that using sandblasting as pre-treatment significantly improved adhesion, especially at higher curing temperatures.

The contact angle measurements showed that an increase in the curing temperature resulted in a transition of the coatings from a hydrophilic to a hydrophobic structure, thus improving the corrosion resistance. The water resistance tests confirmed the effectiveness of the coatings cured at 210°C and 220°C, while the adhesion and performance at lower curing temperatures were found to be inadequate. The moisture resistance test highlighted the embrittlement of coatings at high curing temperatures, which affected adhesion and performance.

The salt spray tests identified the optimum curing conditions for corrosion resistance, with coatings cured at 210°C showing superior performance.

The cycle test, a more aggressive assessment, confirmed the corrosion resistance of Cataphoresis + Geomet321 + ML Black lasting 1512 hours (63 cycles) without red or white rust formation. As a result, 50% superior corrosion resistance was obtained compared to other studies in the literature.

## Article Information Form

### Acknowledgments

The authors would like to thank UZMAN Kataforez for providing laboratory and analysis facilities.

### Funding

The authors have not received any financial support for the research, authorship, or publication of this study.

### Authors' Contribution

Conceptualization, İ.U. and O.Y.; methodology, M.G.; validation, İ.U.; writing—original draft preparation, İ.U.; writing—review and editing, İ.U, M.G, and O.Y; supervision, M.G.; project administration, A.C. All authors have read and agreed to the published version of the manuscript.

### *The Declaration of Conflict of Interest/ Common Interest*

No conflict of interest or common interest has been declared by the authors.

### *The Declaration of Ethics Committee Approval*

This study does not require ethics committee permission or any special permission.

### *The Declaration of Research and Publication Ethics*

The authors of the paper declare that they comply with the scientific, ethical and quotation rules of SAUJS in all processes of the paper and that they do not make any falsification on the data collected. In addition, they declare that Sakarya University Journal of Science and its editorial board have no responsibility for any ethical violations that may be encountered, and that this study has not been evaluated in any academic publication environment other than Sakarya University Journal of Science.

### *Copyright Statement*

Authors own the copyright of their work published in the journal and their work is published under the CC BY-NC 4.0 license.

## References

- [1] G. Koch, "Cost of corrosion," Trends in oil and gas corrosion research and technologies: Production and transmission, Elsevier Inc., A. M. El-Sherik, 2017, pp. 3–30.
- [2] J. Kinugasa, F. Yuse, M. Tsunazawa, M. Nakaya, "Effect of corrosion resistance and rust characterization for hydrogen absorption into steel under an atmospheric corrosion condition," ISIJ International, vol. 56, pp. 459–464, 2016.
- [3] H. Li, Y. He, P. Luo, Y. Fan, H. Yu, Y. Wang, T. He, Z. Li, H. Zhang, "Influence of pulse frequency on Corrosion Resistance and Mechanical Properties of Ni-W/B<sub>4</sub>C Composite Coatings," Colloids

- Surface A Physicochemical Engineering Asp, vol. 629, 127406, 2021.
- [4] A. Karadag, E. Duru, M. Uysal, H. Akbulut, "Tribological performance of Ni-W/PTFE composite coating," vol. 26, no. 4A, pp. 2885–2893, 2022.
- [5] H. Gül, M. Uysal, H. Akbulut, A. Alp, "Effect of PC electrodeposition on the structure and tribological behavior of Ni-Al<sub>2</sub>O<sub>3</sub> nanocomposite coatings," Surface Coating Technology, vol. 258, pp. 1202–1211, 2014.
- [6] Y. Yang, L. Qu, L. Dai, T. S. Kang, M. Durstock, "Electrophoresis coating of titanium dioxide on aligned carbon nanotubes for controlled syntheses of photoelectronic nanomaterials," Advanced Materials, vol. 19, no. 9, pp. 1239–1243, 2007.
- [7] S. M. A. Shibli, B. N. Meena, R. Remya, "A review on recent approaches in the field of hot dip Zinc Galvanizing process," Surface Coating Technology, vol. 262, pp. 210–215, 2015.
- [8] A. R. Marder, "The metallurgy of Zinc-Coated steel," Progress in Materials Science, vol. 45, no. 3, pp. 191–271, 2000.
- [9] H. Cheng Yu, B. Zhen Chen, X. Shi, X. Sun, B. Li, "Investigation of the Trivalent-Chrome Coating on 6063 Aluminum Alloy," Materials Letters, vol. 62, no. 17–18, pp. 2828–2831, 2008.
- [10] P. K. Sinha, R. Feser, "Phosphate coating on steel surfaces by an electrochemical method," Surface Coating Technology, vol. 161, no. 2–3, pp. 158–168, 2002.
- [11] H. Gul, İ. Usta, "Effect of Alumina Concentration on morphology, wear, and corrosion: Electroless Ni-W-P/Al<sub>2</sub>O<sub>3</sub> composite coatings on aluminum surfaces," Journal of Materials Engineering and Performance, vol. 32, no. 13, pp. 6107–6122, 2023.
- [12] A. López-Ortega, R. Bayón, J. L. Arana, "Evaluation of protective coatings for offshore applications. Corrosion and tribocorrosion behavior in synthetic seawater," Surface Coating Technology, vol. 349, pp. 1083–1097, 2018.
- [13] J. R. Lince, "Effective application of solid lubricants in spacecraft mechanisms," Lubricants, vol. 8, p. 74, 2020.
- [14] H. C. Barshilia, "Surface modification technologies for aerospace and engineering applications: Current trends, challenges and future prospects," Transactions of the Indian National Academy of Engineering, vol. 6, no. 2, pp. 173–188, 2021.
- [15] W. Skotnicki, D. Jędrzejczyk, "The Comparative analysis of the coatings deposited on the automotive parts by the cataphoresis method," Materials, vol. 14, no. 20, p. 6155, 2021.
- [16] M. Doerre, L. Hibbitts, G. Patrick, N. K. Akafuah, "Advances in automotive conversion coatings during pretreatment of the Body Structure: A Review," Coatings, vol. 8, no. 11, p. 405, 2018.
- [17] N. Sorour, W. Zhang, E. Ghali, G. Houlachi, "A review of organic additives in Zinc Electrodeposition process" Hydrometallurgy, vol. 171, pp. 320–332, 2017.
- [18] "Home | ZINC. International Zinc Association. (2023, Jul. 17). Zinc essential for modern life [Online]. Available: <https://www.zinc.org/>
- [19] N. Rawal. (2023). The Characteristics, Toxicity and Effects of Cadmium [Online]. Available: <https://www.researchgate.net/publication/305778858>
- [20] R. Ding, S. Chen, J. Lv, W. Zhang, X. Zhao, J. Liu, X. Wang, T. Gui, B. Li, Y.

- Tang, W. Li, "Study on graphene modified organic anti-corrosion coatings: A comprehensive review," *Journal of Alloys and Compounds*, vol. 806, pp. 611–635, 2019.
- [21] B. Philip (2011). Evaluation of Corrosion in Crevices in Screw Joints Mats Thörnqvist [Online]. Available: <https://www.diva-portal.org/smash/get/diva2:441388/FULLTEXT01.pdf>
- [22] D. Zhmurkin, "Corrosion Resistance of Bolt Coatings Technical Paper," Tyco Electronics Harrisburg, PA, pp. 1-7, 2009.
- [23] Benseler. (2023). New Dip-Spin System for Zinc Flake Coatings on Rack Parts All-Over Coating [Online]. Available: <https://www.benseler.de/en/verfahren/beschichtung/geomet.php>
- [24] "Geomet Coating. (2023). Keys & Clamps." [Online]. Available: <https://www.keytechno.com/service/geom-et-coating/>
- [25] K. Westphal, "An optimized coating system for fasteners with metric threads," *ATZ Worldwide*, vol. 107, no. 5, pp. 8–10, 2005.
- [26] R. B. Egêa, A. Primolini, B. I. Da Maia, "Development of friction coefficient controller for E-coat (KTL)," *SAE Technical*, 2018-36-0200, 2018.
- [27] B. Oleksiak, K. Kołtało, R. Poloczek, "Application methods and selected properties of Zinc Flake coatings," *Metalurgija*, vol. 60, pp. 162–164, 2021.
- [28] M. R. Isa, O. S. Zaroog, M. A. Yunus, V. R. Sanny Bavu, N. Rosmi, "Effect of sandblasting process on mechanical properties of ASTM A516 Grade 70 Steel," *Key Engineering Materials*, vol. 765, pp. 222–226, 2018.
- [29] A. Rudawska, I. Danczak, M. Müller, and P. Valasek, "The effect of sandblasting on surface properties for adhesion," *International Journal of Adhesion and Adhesives*, vol. 70, pp. 176–190, 2016.
- [30] B. Herbáth, K. Kovács, M. Jakab, É. Makó, "Crystal structure and properties of Zinc Phosphate Layers on aluminium and steel alloy surfaces," *Crystals*, vol. 13, p. 369, 2023.
- [31] L. Kwiatkowski, "Phosphate coatings porosity: Review of new approaches," *Surface Engineering*, vol. 20, no. 4, pp. 292–298, 2013.
- [32] M. Kiliç, L. Akyalcın, "Kataforez kaplamalı çelik yüzeylere uygulanan dubleks kaplamanın korozyon dayanım performansı üzerindeki etkisinin incelenmesi," *Eskişehir Osmangazi Üniversitesi Mühendislik ve Mimarlık Fakültesi Dergisi*, vol. 30, pp. 68–78, 2022.
- [33] A. Ş. Yargıç, B. Eren, N. Özbay, "Enhancement of coating features by supporting Zinc-Based coating with cataphoresis process: Effect of acidity and coating thickness on the coating Quality," *Journal of Polytechnic*, pp. 1, 2023.
- [34] Yellow Powder Coating (2023). PPG Powder Coating Colors | PPG Powder Coatings [Online]. Available: <https://powdercoatings.ppg.com/products/pctz39104-yellow>
- [35] S. J. García, J. Suay, "A comparative study between the results of different electrochemical techniques (EIS and AC/DC/AC) application to the optimisation of the cataphoretic and curing parameters of a primer for the automotive industry," *Progress in Organic Coatings* vol.59, pp. 251–258, 2007.
- [36] S. J. García, M. T. Rodríguez, R. Izquierdo, J. Suay, "Evaluation of cure temperature effects in cataphoretic automotive primers by electrochemical techniques," *Progress in Organic Coatings*, vol.60, no.4, pp. 303–311, 2007.

- [37] “Cross Hatch Method. (2023). [Online]. Available: <https://www.elcometer.com/en/cross-hatch-method>
- [38] “Adhesion tests (2023). [Online]. Available: [https://www.substech.com/dokuwiki/doku.php?id=adhesion\\_tests](https://www.substech.com/dokuwiki/doku.php?id=adhesion_tests)
- [39] “ASTM D 870: 2002 Standard (2023). Practice for testing water resistance.” [Online]. Available: [https://infostore.saiglobal.com/en-us/standards/astm-d870-02-151549\\_SAIG\\_ASTM\\_ASTM\\_357357/](https://infostore.saiglobal.com/en-us/standards/astm-d870-02-151549_SAIG_ASTM_ASTM_357357/)
- [40] “MIL-STD-810 Test Method 507 Humidity-Crystal group.” (2023). [Online]. Available: <https://www.crystalrugged.com/mil-std-810-test-method-507-humidity/>
- [41] DIN EN ISO 9227 – (2023) European Standards. [Online]. Available: <https://www.en-standard.eu/din-en-iso-9227-corrosion-tests-in-artificial-atmospheres-salt-spray-tests-iso-9227-2022/>
- [42] SIST EN ISO 9227:2006 – (2023) Corrosion Tests in Artificial Atmospheres - Salt Spray Tests [Online]. Available: <https://standards.iteh.ai/catalog/standards/sist/6e82d425-e4fd-4579-a86d-d94eddd1cb36/sist-en-iso-9227-2006>
- [43] B. Chatterjee, (2017) “Science and industry of processes for Zinc-based coatings with improved properties,” *Jahrbuch Oberflächentechnik Band*, pp 1-30, [Online]. Available: <https://www.researchgate.net/publication/311793888>
- [44] L. Zaretskiy, “Modified silicate binders new developments and applications,” *International Journal of Metal Casting*, vol. 10, no. 1, pp. 88–99, 2016.
- [45] L. Zaretskiy, “Modified Silicate Binders New developments and applications,” *International Journal of Metal Casting*, vol. 10, no. 1, pp. 88–99, 2016.
- [46] L. Feng, H. Zhang, “Superhydrophobic aluminium alloy surface: Fabrication, structure, and corrosion resistance,” *Physicochemical Engineering Aspects*, vol. 441, pp. 319–325, 2014.
- [47] B. Tylkowski, I. Tsibranska, “Overview of main techniques used for membrane characterization,” *Journal of Chemical Technology and Metallurgy*, vol. 50, 1 pp. 3-12, 2015.
- [48] M. Mantel, J. P. Wightman, “Influence of the surface chemistry on the wettability of stainless steel,” *Surface and Interface Analysis*, vol. 21, pp. 595–605, 1994.
- [49] A. R. Luz, L. S. Santos, C. M. Lepienski, P. B. Kuroda, “Characterization of the morphology, structure and wettability of phase dependent lamellar and nanotube Oxides on Anodized Ti-10Nb Alloy,” *Applied Surface Science*, vol. 448, pp. 30–40, 2018.
- [50] D. Crotty, “Zinc alloy plating for the automotive industry,” *Metal Finishing*, vol. 94, pp. 56-58, 1996.
- [51] Teknorot (2023). Cataphoresis [Online]. Available: <https://www.teknorot.com/en/cataphoresis/>
- [52] GEOMET® (2023) Protection Principals,. [Online]. Available: [www.nofmetalcoatings.com](http://www.nofmetalcoatings.com)